Materials Science & Engineering C 97 (2019) 406–411

Contents lists available at ScienceDirect

Materials Science & Engineering C

journal homepage: www.elsevier.com/locate/msec

A unique FRET approach toward detection of single-base mismatch DNA in *BRCA1* gene

Yasaman-Sadat Borghei[a], Morteza Hosseini[a,*], Mohammad Reza Ganjali[b,c], Huangxian Ju[d,*]

[a] Department of Life Science Engineering, Faculty of New Sciences & Technologies, University of Tehran, Tehran, Iran
[b] Center of Excellence in Electrochemistry, Faculty of Chemistry, University of Tehran, Tehran, Iran
[c] Biosensor Research Center, Endocrinology & Metabolism Molecular-Cellular Sciences Institute, Tehran University of Medical Sciences, Tehran, Iran
[d] State Key Laboratory of Analytical Chemistry for Life Science, Department of Chemistry, Nanjing University, Nanjing 210023, China

ARTICLE INFO

Keywords:
Fluorescence analysis
DNA
FRET
Quantum dots
Silver nanocluster
Single-base mismatch

ABSTRACT

Early detection of mutation carriers in predisposing genes such as *BRCA1* plays an important role in disease prevention. This work developed a quantum dots-based (QDs-based) fluorescence resonance energy transfer (FRET) technique for the detection of single-base mismatch DNA in *BRCA1* gene. The FRET between QDs as the donor and silver nanocluster (AgNCs) as the acceptor was designed by the strong interaction between CdTe QDs with appropriate size and dsDNA through binding to its major groove. The dsDNA was formed by the hybridization of ssDNA labeled to AgNCs with target DNA, which introduced CdTe QDs into the major grooves to place the AgNCs in close proximity to the QDs. The complementary and single-base mismatch DNA led to obviously different FRET signals. The FRET signal linearly correlated to the concentration of single-base mismatch DNA in the range of 1.5×10^{-10}–1.0×10^{-6} mol L^{-1}. The proposed method showed a detection limit of 80 pmol L^{-1} and the sensitivity comparable to the previously reported assays, indicating promising potential for single nucleotide polymorphisms diagnosis in clinical application.

1. Introduction

Breast cancer (BC) is the most common cancer in females all over the world. *BRCA1* and *BRCA2* gene mutations comprise the most important BC susceptibility [1]. Germline mutations in the BRCA1/2 genes are the most common cause of hereditary breast cancer [2]. BRCA1 is a tumor suppressor gene and participates in gene regulation processes following DNA damage. Over 2000 different mutations have been described in BRCA1/2 genes involving deletions, insertions, and many single nucleotide polymorphisms (SNP) in coding or noncoding sequences. The BRCA1 gene mutations damages DNA and elevates the risk of BC [3]. Thus the accurate detection of single-nucleotide variation in DNA has attracted much attention due to the diagnostic need of mutation related diseases, since the detection method toward BRCA1/2 gene mutations was developed [4].

SNP is the single nucleotide variation in a defined genetic location and occurs in human genome at a frequency of approximately 1 in every 1000 bases [5–8]. As genetic markers, SNPs can be used to trace inheritance patterns associated with specific diseases such as cancer [5]. SNP detection is important to biomedical research, the prediction of disease resistance, and developing pharmacy products and thus a fast, reliable and inexpensive sensor is required for use in genetic variations diagnostics. Current methods for SNP detection such as primer extension, enzymatic ligation, enzymatic cleavage, molecular beacon, denaturing gel electrophoresis, TaqMan assay during PCR reaction, typically require enzymatic reactions and labeled probes [9–11]. With the growth of the "-omics" such as functional genomics and the demands of disease diagnosis, efficient analytical approach to monitor SNP in a systematic manner is recently becoming the choice for such a task due to its inherent merits of simple operational procedures, particularly in real time and in situ identification through conjunction with optical spectroscopy.

Fluorescent nanomaterials, such as quantum dots (QDs) and Ag nanoclusters (NCs) (collections of ~2 to 30 silver atoms), have become useful reporters for DNA detection [5,12]. Few-atom noble-metal NCs (collections of ~2 to 30 atoms) are a new class of fluorophores and exhibit strong and size-dependent fluorescence emission [13–15]. AgNCs can be easily synthesized using a number of ligands [14,15], such as DNA oligomers [16–19], as stabilization agents. They have gained attention due to their unique optical properties and potential applications in the fields of optical sensing [20]. These optical methods are attractive because they are fast, simple, cheap and can be easily

* Corresponding authors.
E-mail addresses: smhosseini@khayam.ut.ac.ir (M. Hosseini), hxju@nju.edu.cn (H. Ju).

https://doi.org/10.1016/j.msec.2018.12.049
Received 5 February 2018; Received in revised form 10 October 2018; Accepted 15 December 2018
Available online 17 December 2018
0928-4931/

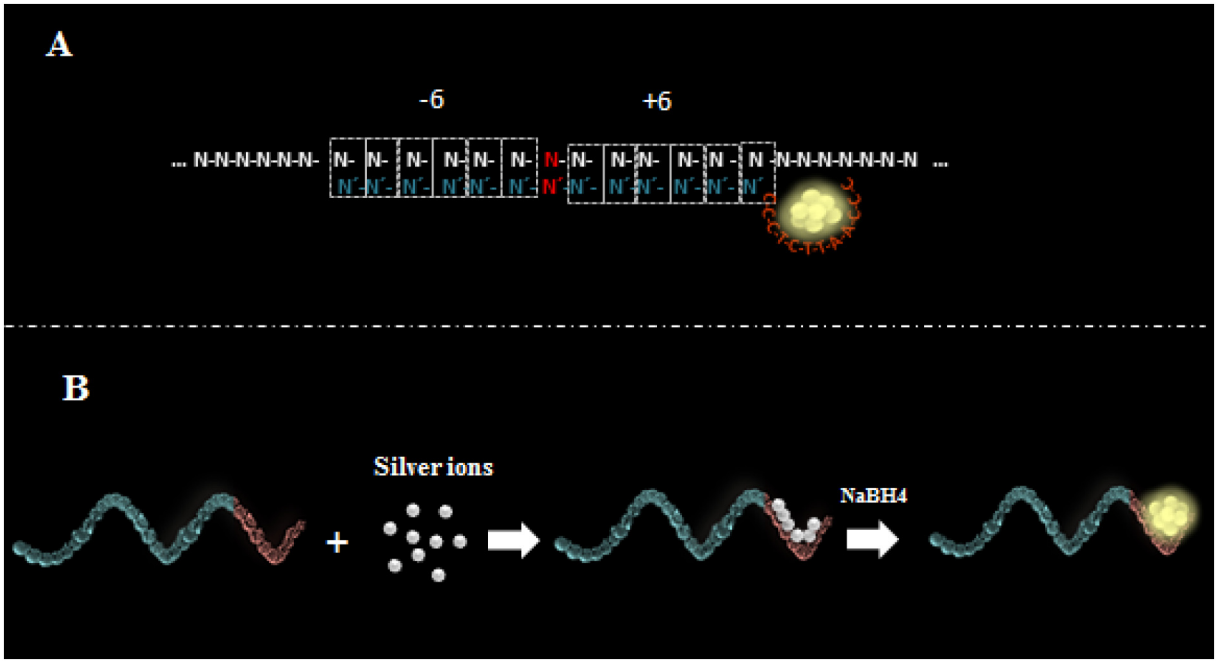

Scheme 1. (A) Schematic shows mismatch locus and probe design and (B) construction of DNA sensors with DNA templated AgNCs (DNA/AgNCs) fluorescent probe.

monitored without any advanced instruments. Among these methods, fluorescence resonance energy transfer (FRET), which occurs between two close molecules (donor and acceptor), is a technique to investigate short distance-dependent interactions between the donor and acceptor [21].

In view of the superior characteristics of quantum dots (QDs) over molecular dyes, including feature size-tuneable fluorescence and interaction-dependent fluorescence transduction efficiency. These features allow for selective detection of a multitude of compounds, and the strong interaction between CdTe QDs with appropriate size and dsDNA through binding to its major groove [21,22]. This work designs a fluorescence resonance energy transfer (FRET) system to develop a novel method for specific identification of single mismatched base and SNP detection. For this purpose, a DNA probe strand was designed containing a T and C bases-abundant end for preparation of encapsulated silver nanoclusters (NCs) (Scheme 1) and a target DNA recognition sequence at another end. The DNA-AgNCs as a nanosensor can be conveniently prepared by the adsorption of Ag^+ on the T and C bases-abundant scaffold and then reduction with reductant (Scheme 1A). Using CdTe QDs as the donor, a FRET system is constructed through introducing the QDs into major grooves of dsDNA formed via the specific hybridization of DNA-AgNCs with target DNA strand, which introduces the QDs and AgNCs (the acceptor) in close proximity for detection of SNP quantitatively (Scheme 2). The proposed method shows excellent performance and promising potential for clinical application.

2. Experimental

2.1. Apparatus

Absorption spectra were determined using Perkin-Elmer lambda 25 spectrometer. All fluorescence measurements were monitored using a Perkin Elmer LS-45 fluorescence spectrometer with a xenon lamp as source of excitation, while the spectral band widths of monochromators for excitation and emission were 10 nm (Buckinghamshire, UK). The size and morphology of CdTe QDs and DNA-AgNCs were measured by transmission electron microscope (TEM) (Zeiss, EM10C, 80 kV, Germany).

2.2. Materials and reagents

All of the following oligonucleotide strands were synthesized by Shanghai Generay Biotech Co. (Shanghai, China). All DNA samples were purified by PAGE and prepared with TE buffer (1 M Tris-HCl containing 0.5 M EDTA).

DNA labeled to AgNC: 5′-ACCTGCGAAATCCCCTCTTAACCC-3′

Wild type target: 5′-TCTGATGTGCTTTGTTCTGGATTTCGCAGGTC CTCAAGGGCAGA AGAGTCACTTATG-3′

Mutant target (SNP ID: R1443X): 5′-TCTGATGTGCTTTGTTCTGGA TTTCACAGGTCC TCAAGGGCAGAAGAGTCACTTATG-3′

Non-complementary target: 5′-TCCGCCCAGGTCA-3′

Cadmium chloride hydrate, tellurium powder, silver nitrate ($AgNO_3$), sodium borohydride ($NaBH_4$) were purchased from Merck. All chemicals used were of analytical grade or of the highest purity available. Deionized water with a resistivity greater than 18 MΩ cm was acquired from a Millipore Milli-Q system.

2.3. Preparation of DNA-AgNCs fluorescent probe

DNA-AgNCs were synthesized according to a previous report [17] with minor modification. 6 μL of 1 mM $AgNO_3$ solution was added to 10 μL of 100 μM DNA in phosphate buffer (20 mM, pH 7.5) to provide a Ag^+-to-DNA molar ratio of 6:1. After incubation for 30 min in an ice bath, this mixture was reduced by adding freshly prepared $NaBH_4$ (1 mM, 6 μL) to react in an ice bath for 1 h. The molar ratios of Ag-DNA-$NaBH_4$ in the solution were 6:1:6. The reaction mixture was kept in the dark at room temperature for 12 h before use. The AgNCs exhibited a fluorescence emission peak at 525 nm when excited at 425 nm (Fig. S1A).

2.4. CdTe quantum dots synthesis

The experimental procedure was performed according to Borghei et al. [17]. In brief, $CdCl_2$ (0.4 mmol) and thioglycolic acid (TGA) (1.4 mmol) were dissolved in 80 mL distilled water with pH adjusted to 10.0 using NaOH solution. Next, sodium borohydrate (0.8 mmol) and

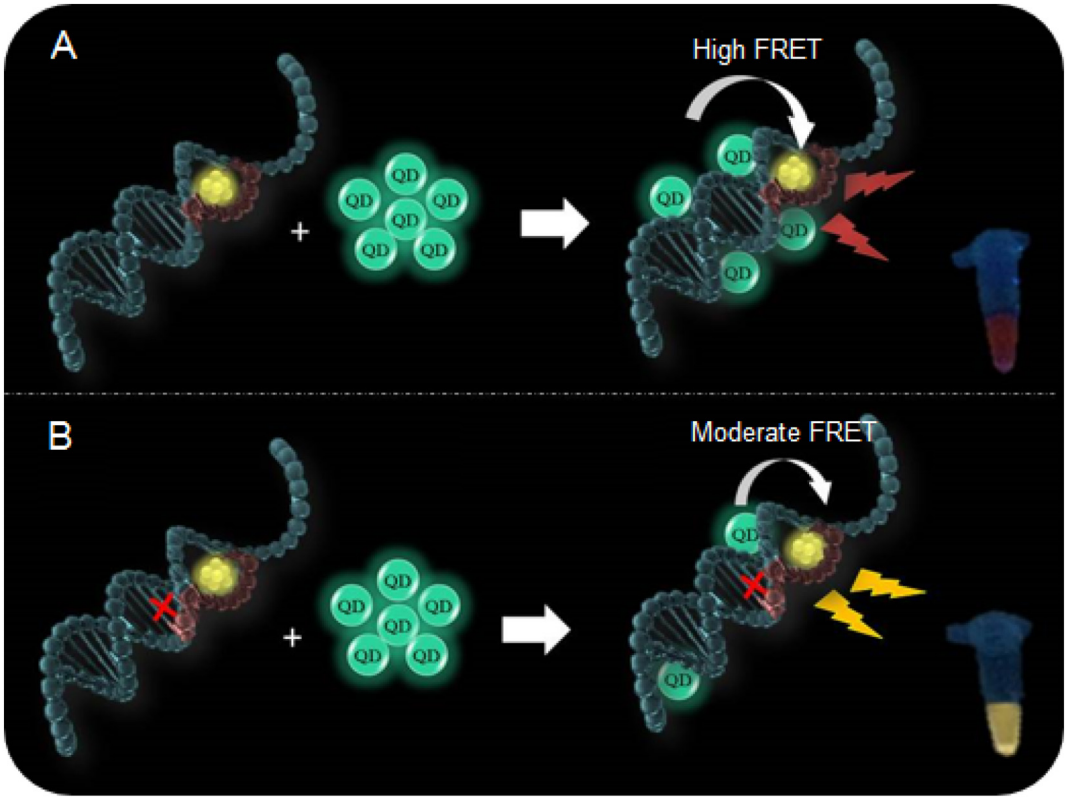

Scheme 2. Schematic representation of the complex probe (ssDNA/templated-silver nanocluster) detecting target DNA, in the presence of the complementary (A) and single-base mismatch (B) DNA.

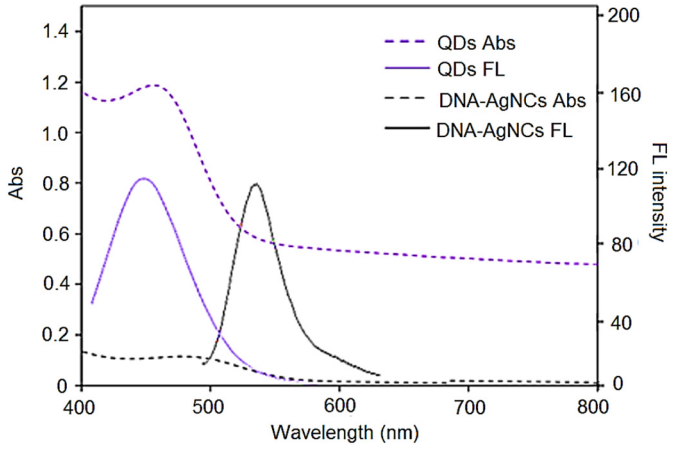

Fig. 1. UV–vis and fluorescence emission spectrum of CdTe QDs and DNA/AgNCs.

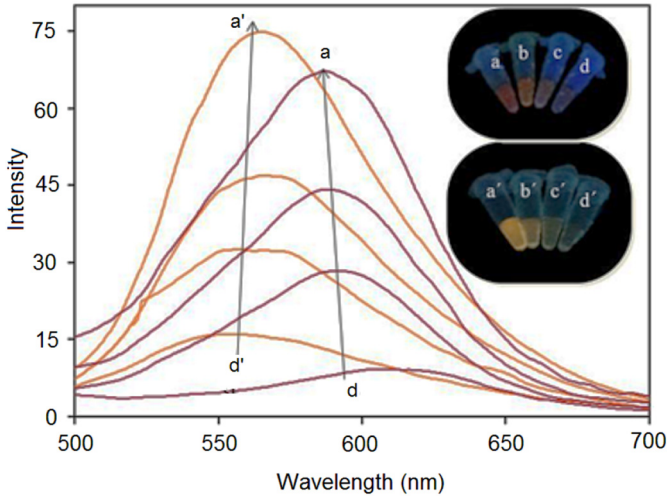

Fig. 2. Emission spectra of QDs@dsDNA-AgNCs formed by mixing DNA-AgNCs with wild type (red line) and mutant type (orange line) targets at 3×10^{-10}, 1.5×10^{-9}, 1.5×10^{-8} and 1.5×10^{-6} M (from d and d′ to a and a′) and then CdTe QDs solution. Inset: Colour change under UV radiation at different concentrations of wild type and mutant type DNA. (For interpretation of the references to colour in this figure legend, the reader is referred to the web version of this article.)

Te powder were diluted in 10 mL distilled water in a flask, with vigorous stirring under argon flow. The mixture was heated to 80 °C to get a clear red NaHTe solution. Cd-TGA solution was heated at 100 °C under argon flow in a 250 mL three-neck flask. Then the freshly prepared NaHTe solution (4.0 mL) was added to the flask, and the resulting solution was refluxed at 100 °C for 2 h. The characterization of CdTe quantum dots was carried out through transmission electron microscopy and spectrofluorometer.

2.5. Agarose gel electrophoresis analysis of DNA-QDs interaction

Agarose gel (3% v/v, high melt, medium fragments, Chemos CZ, s.r.o., Prague, Czech Republic) was prepared with 1 × TAE buffer (40 mM Tris, 20 mM acetic acid and 1 mM ethylenediaminetetraacetic acid). 5 μL of samples were prepared with 5% (v/v) bromophenol blue and 3% (v/v) glycerol and loaded into a gel. The electrophoresis was run at 60 V and 6 °C for 45 min and visualized by UV transilluminator (312 nm). The intercalation of QDs into the DNA structure also led to the change in the electrophoretic behavior of the DNA-QDs complexes.

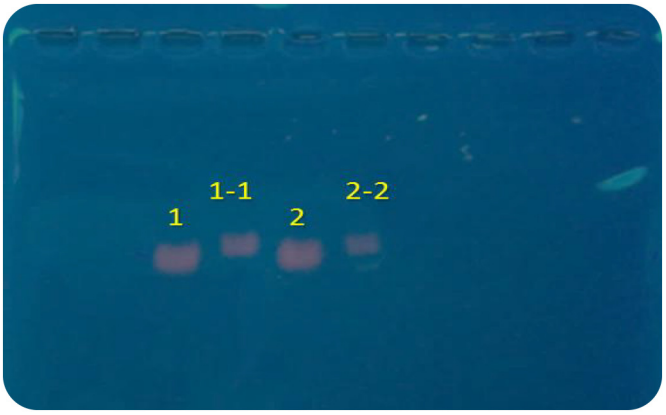

Fig. 3. Gel electrophoresis of dsDNA-AgNCs formed by incubating DNA-AgNCs with (1) mutant type and (2) wild type target, and QDs@dsDNA-AgNCs formed after mixing QDs solution with (1-1) mutant type and (2-2) wild type dsDNA-AgNCs.

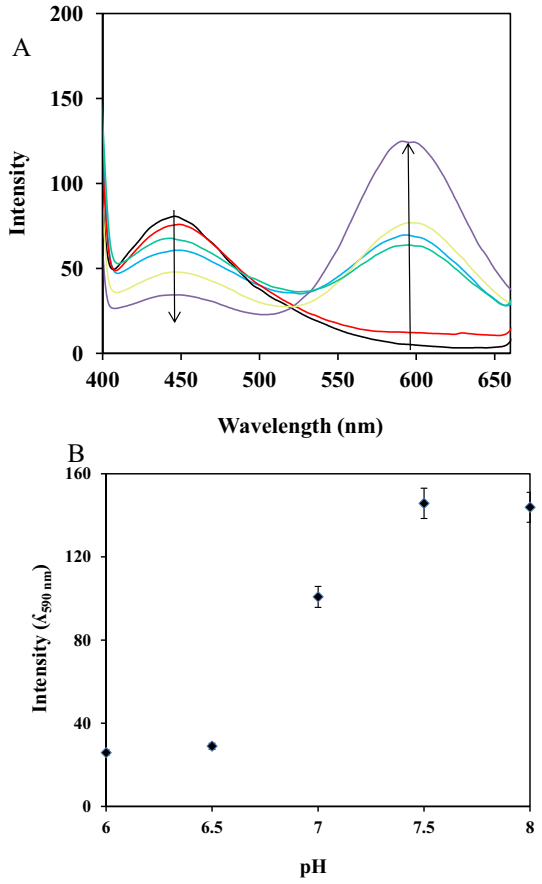

Fig. 4. (A) Fluorescence emission spectra of CdTe QDs upon addition of dsDNA-AgNCs at 0, 1.0, 5.0, 10, 15 and 20 nM in the presence of wild type DNA, and (B) effect of pH (from 6.0–8.0) on fluorescence intensity.

2.6. Hybridization and fluorescence detection

In order to determine the hybridization effects of complementary and non-complementary (single-base mismatch) targets on fluorescence intensity, different concentrations of target, single-base mismatch DNA in *BRCA1* gene, were added to obtain DNA-AgNCs solution. The hybridization was carried out by incubation for 1 h at 37 °C. Afterward, 12 μL of QDs (2.0×10^{-8} mol L^{-1}) was added to 38 μL reaction solution to examine the FRET phenomenon. All fluorescence measurements were carried out at room temperature.

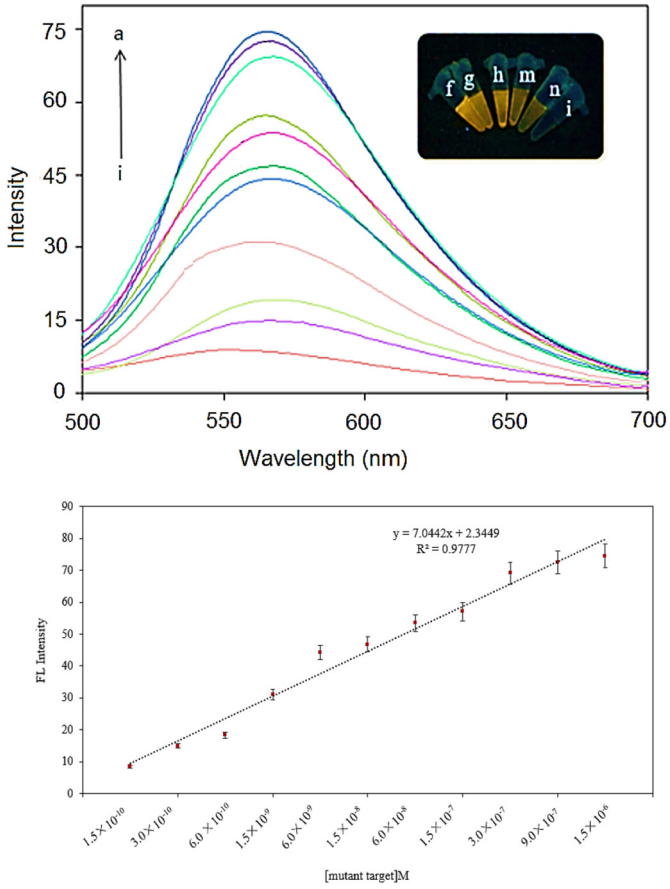

Fig. 5. Fluorescence spectra of QDs@dsDNA-AgNCs formed at increasing concentration of mutant type DNA with single base mismatch at 1.5×10^{-10}, 3.0×10^{-10}, 6.0×10^{-10}, 1.5×10^{-9}, 6.0×10^{-9}, 1.5×10^{-8}, 6.0×10^{-8}, 1.5×10^{-7}, 3.0×10^{-7}, 9.0×10^{-7}, 1.5×10^{-6} M.

3. Results and discussion

3.1. FRET between CdTe and DNA/AgNCs

The selection of QDs with a size appropriate to DNA-AgNCs as an energy-transfer pair permits minimal spectral cross-talk between donor and acceptor emissions. The spectral characteristics of the designed FRET system were firstly studied in Fig. 1. The absorption spectra of the DNA-AgNCs and CdTe QDs showed obvious overlap of absorption bands in the wavelength range of 430–530 nm. The fluorescence emission peak of CdTe QDs with excitation at 370 nm occurred at around 450 nm, which was far from the emission peak of DNA-AgNCs at 525 nm upon excitation at 425 nm. The broad absorption band of DNA-AgNCs contributed to flexibility in choosing a suitable excitation wavelength to excite the QDs, and the great separation of two emission peaks and the minimum absorption of DNA-AgNCs at the excitation wavelength of the QDs to eliminate the direct acceptor excitation allowed for FRET-based target detection with low background [24–28].

3.2. Characterization of DNA-AgNCs and CdTe quantum dots

During the incubation of the silver salt with the oligonucleotide, the Ag^+ ions bound to the cytosine bases at N3 site. The close proximity of several Ag^+ ions in this precursor complex favored the generation of AgNCs after reduction with $NaBH_4$ (Scheme 1B). Transmission electron microscopy was used to observe the size and morphology of synthesized

Table 1
Detection performance comparison of our strategy in one-base mismatch (or SNP) detection with other methods by using nanotechnology.

Nano-based	Method	Detection limit	References
Silver nanocluster	Fluorescence intensity	1.3 nM	[29]
Gold magnetic nanoparticles	Combining ARMS-PCR with lateral flow assay (LFA)	5 ng	[30]
Nanochannel-array	Electrochemically monitoring the diffusion flux of ferricyanide probe	–	[31]
Gold nanorod arrays	localized surface plasmon resonances (LSPR)	Down to 10 nM	[32]
Magnetic beads (MBs)-based rolling circle amplification combined with gold nanoparticles (AuNPs)	Inductively coupled plasma mass spectrometry (ICP-MS)	0.1 fM	[33]
Gold nanoparticles (GNPs) uniformly deposited in a nanohemisphere array	Cyclic voltammetry detection	–	[34]
Graphene oxide-chitosan nanocomposite	Electrochemical DNA biosensor	10 fM	[35]
AgNCs-QDs	Fluorescence resonance energy transfer (FRET)	80 pM	In this work

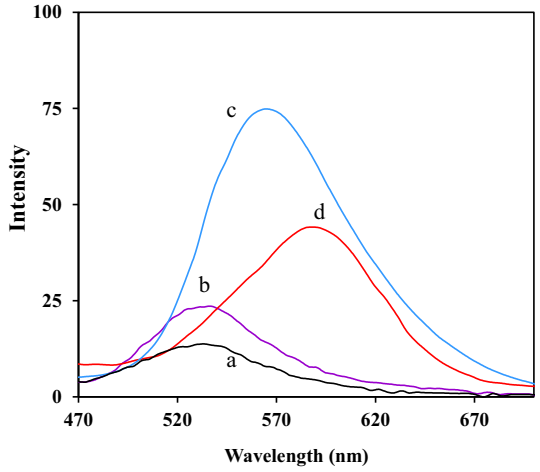

Fig. 6. Selectivity of the proposed method for single-base mismatched DNA in phosphate buffer (pH = 7.5), (a) blank, (b) non-complementary DNA, (c) single-base mismatched sequence, and (d) complete complementary sequence.

AgNCs with DNA template. The TEM image indicated that AgNCs with an average diameter of about 2–3 nm were formed on DNA scaffolds, and the optical properties of the DNA-AgNCs were dependent on the sequence of the DNA target (complementary or single-base mismatch sequence) (Fig. S1). Upon excitation at 425 nm, DNA-AgNCs showed a maximum emission signal at 525 nm (Fig. S1A). Although the fluorescence emission peaks from AgNCs in the formed double helix structure of complementary or single-base mismatch sequence/DNA-AgNCs occurred at the same wavelength, their peak intensities were much different due to the effect of DNA structure on fluorescence transduction efficiency.

3.3. Characterization of CdTe quantum dots

QDs are known as size-dependent nanomaterials. The size is controllable during the synthesis process, which can provide a desired absorbance and emission spectra for the specific application. CdTe QDs with desired size (2 nm) were synthesized according to the method described elsewhere [17]. Their size-distribution was shown in TEM image (Fig. S2). The majority of the nanoparticles were 2 nm in diameter, which showed the blue-green fluorescence emission under UV light. The relative quantum yield (QY) of CdTe/MPA QD emitting at 450 nm and DNA-AgNCs at 525 nm were examined to be 52% and 4.4% respectively by comparing with fluorescence emission of fluorescein in water.

3.4. Effect of QDs-dsDNA interaction on fluorescence wavelength

The conjugation of QDs and DNA-AgNCs relies on QDs-DNA interaction [23–26]. After the dsDNA-AgNCs were formed by mixing mutant type or wild type target with DNA-AgNCs and incubating for 1 h at 37 °C, they were mixed with CdTe QDs solution, which led to the implantation of QDs to the major grooves of the formed dsDNA to generate FRET signal. The FRET signal intensity increased with the increasing concentration of target, both mutant type and wild type DNA (Fig. 2), which produced a simple strategy for quantitative detection of target concentration. The wild type DNA target could generate strong FRET signal, while the QDs dispersed randomly in the system in the case of single-base mismatch, and a Förster distance R_0 was not satisfied, leading to moderate FRET. Interestingly, the emission wavelength depended on the target sequence. In other words, the FRET signal was dependent on the DNA-QDs interaction. After excitation by the excited CdTe QDs produced at 370 nm, the maximum emission wavelength of normal target was at 590 nm, and that of mutant target DNAs was at 575 nm, which allowed qualitatively distinguishing between normal and wild type DNA sample.

Gel electrophoresis was employed to verify the DNA-QDs interaction (Fig. 3). Lanes 1 and 2 were injected with the dsDNA-AgNCs formed by mutant and wild type target DNA, respectively. After these dsDNA-AgNCs were mixed with QDs at a molar ratio of 1:1, the lanes 1-1 and 2-2 showed the pale colour probably due to the fact that DNA-QDs interaction was preventing the DNA staining, and QDs@dsDNA-AgNCs complexes could be detected from the delayed electrophoretic migration.

3.5. Optimization of experiment conditions

The efficiency of FRET was greatly dependent on the amount of dsDNA-AgNCs added in CdTe QDs, and the pH of detection solution. Fig. 4A shows the fluorescent emission spectra of the mixture of QDs@dsDNA-AgNCs, CdTe QDs, and dsDNA-AgNCs formed at different dsDNA-AgNCs concentrations in the presence of complementary DNA target in phosphate buffer (10 mM, pH 7.5). With the increasing amount of dsDNA-AgNCs in the mixture, the FRET signal at about 590 nm increased, while the fluorescence emission peak of CdTe QDs at around 450 nm decreased, indicating that more QDs@dsDNA-AgNCs were produced to quench the fluorescence of CdTe QDs. These fluorescence changes further confirmed the FRET between the donor and acceptor pairs.

The effect of pH on the fluorescence intensity was also studied over a range of 6.0–8.0. The maximum intensity was obtained at pH 7.5 (Fig. 4B). Significantly, modest responses could still be achieved at pH values of 6.0–8.0, showing that this assay could be utilized under a range of pH values around physiological conditions. It has been suggested that in this pH (pH 7.5) DNA can be rapidly adsorbed onto negatively charged thioglycolic acid capped CdTe QDs surface to act as a coating and stabilizer. While very alkaline or very acidic conditions cause QDs damage.

3.6. Analytical performance

In order to examine the analytical performance of the designed method for detecting the complementary and non-complementary target, the fluorescence spectra with excitation at 370 nm were recorded after 20 nM CdTe QDs was added in the detection solution containing DNA-AgNCs and target sample. Upon the increase in mutant target concentration from 1.5×10^{-10} M to 1.5×10^{-6} M, the fluorescence intensity of QDs-AgNCs with excitation at 370 nm showed linear increase (Fig. 5). The regression coefficient (R) of the linear curve for mutant type sequence was 0.995 with the detection limit of 80 pM. The relative standard deviation for 5 measurements of 1.5×10^{-8} M non-complementary target (single base mismatch) was 2.1%. The sensitivity of this assay was comparable to the previously reported assays (Table 1) [29–35].

The selectivity of this method was further investigated by examining the fluorescence responses of the nanosensor toward perfectly matched target DNA, one-base mismatched target DNA, non-complementary target DNA and blank at the same concentration (1.5×10^{-7} M). As shown in Fig. 6, all of these results indicated the high selectivity for detection of single base mismatch in this system. Therefore, the label-free and sensitive detection method for one-base mismatched sequence could be of great potential for SNP diagnosis in clinical application.

4. Conclusion

This work reports a FRET-based technique for the detection of single-base mismatch DNA. The FRET fluorescence between QDs and AgNCs in the presence of complementary and single-base mismatch DNA shows different efficiencies due to different interactions of QDs with the formed DNA structures, which leads to the strategy for both quantitative detection of target concentration and qualitatively distinguishing between normal and wild type DNA sample. The quantitative detection method shows excellent performance without help of any signal amplification, indicating great potential for SNP diagnosis in clinical application.

Acknowledgment

The authors thank the research Council of University of Tehran (28645/01/02) and National Natural Science Foundation of China (21635005, 21827812) for financial support of this work.

Appendix A. Supplementary data

Supplementary data to this article can be found online at https://doi.org/10.1016/j.msec.2018.12.049.

References

[1] F. Karami, P. Mehdipour, A comprehensive focus on global spectrum of *BRCA1* and *BRCA2* mutations in breast cancer, Biomed. Res. Int. 2013 (2013) 1–21.
[2] B. Park, J.Y. Sohn, K.A. Yoon, K.S. Lee, E.H. Cho, M.C. Lim, M.J. Yang, S.J. Park, M.H. Lee, S.Y. Lee, Y.J. Chang, D.O. Lee, S.Y. Kong, E.S. Lee, Characteristics of BRCA1/2 mutations carriers including large genomic rearrangements in high risk breast cancer patients, Breast Cancer Res. Treat. 163 (2017) 139–150.
[3] N. Xu, Y. Yang, D. Zhou, C. Zhong, H. Gao, C. Ye, BRCA1 gene mutation rate in breast cancer patients and its clinical significance, Int. J. Clin. Exp. Pathol. 10 (2017) 603–610.
[4] J. Ma, J. Yang, W. Jian, X. Wang, D. Xiao, W. Xia, L. Xiong, D. Ma, A novel loss-of-function heterozygous *BRCA2* c.8946_8947delAG mutation found in a Chinese woman with family history of breast cancer, J. Cancer Res. Clin. Oncol. 143 (2017) 631–637.
[5] J. Ma, J. Yang, W. Jian, X. Wang, D. Xiao, W. Xia, L. Xiong, D. Ma, A fluorescence light-up Ag nanocluster probe that discriminates single-nucleotide variants by emission color, J. Am. Chem. Soc. 134 (2012) 11550–11558.
[6] N. Moran, D.M. Bassani, J.P. Desvergne, S. Keiper, P.A.S. Lowden, J.S. Vyle, J.H.R. Tucker, Detection of a single DNA base-pair mismatch using an anthracenetagged fluorescent probe, Chem. Commun. (2006) 5003–5005.
[7] N. Tian, Y. Tang, Q.H. Xu, S. Wang, Single base pair mismatch detection using cationic conjugated polymers through fluorescence resonance energy transfer, Macromol. Rapid Commun. 28 (2007) 729–732.
[8] K. Chang, S. Deng, M. Chen, Novel biosensing methodologies for improving the detection of single nucleotide polymorphism, Biosens. Bioelectron. 66 (2015) 297–307.
[9] K. Ma, Q. Cui, G. Liu, F. Wu, S. Xu, Y. Shao, DNA abasic site-directed formation of fluorescent silver nanoclusters for selective nucleobase recognition, Nanotechnology 22 (2011) 305502.
[10] H. Deng, W. Shen, Z. Gao, Colorimetric detection of single nucleotide polymorphisms in the presence of 103-fold excess of a wild-type gene, Biosens. Bioelectron. 68 (2015) 310–315.
[11] J.W. Jian, C.C. Huang, Colorimetric detection of DNA by modulation of thrombin activity on gold nanoparticles, Chem. Eur. J. 17 (2011) 2374.
[12] G.Y. Lan, W.Y. Chen, H.T. Chang, One-pot synthesis of fluorescent oligonucleotide Ag nanoclusters for specific and sensitive detection of DNA, Biosens. Bioelectron. 26 (2011) 2431–2435.
[13] W. Guo, J. Yuan, Q. Dong, E. Wang, Highly sequence-dependent formation of fluorescent silver nanoclusters in hybridized DNA duplexes for single nucleotide mutation identification, J. Am. Chem. Soc. 132 (2010) 932–934.
[14] Y.S. Borghei, M. Hosseini, M. Khoobi, M.R. Ganjali, Novel fluorometric assay for detection of cysteine as a reducing agent and template in formation of copper nanoclusters, J. Fluoresc. 27 (2017) 529–536.
[15] Y.S. Borghei, M. Hosseini, M.R. Ganjali, S. Hosseinkhani, A novel BRCA1 gene deletion in human breast carcinoma MCF-7 cells through FRET between quantum dots and silver nanoclusters, J. Pharm. Biomed. Anal. 15 (2018) 81–88.
[16] J.M. Obliosca, C. Liu, R. Austin Batson, M.C. Babin, J.H. Werner, H.C. Yeh, DNA/RNA detection using DNA-templated few-atom silver nanoclusters, Biosensors 3 (2013) 185–200.
[17] Y.S. Borghei, M. Hosseini, M.R. Ganjali, Fluorometric determination of microRNA via FRET between silver nanoclusters and CdTe quantum dots, Microchim. Acta 184 (2017) 4713–4721.
[18] Y.S. Borghei, M. Hosseini, M.R. Ganjali, S. Hosseinkhani, Label-free fluorescent detection of microRNA-155 based on synthesis of hairpin DNA-templated copper nanoclusters by etching (top-down approach), Sensors Actuators B Chem. 248 (2017) 133–139.
[19] Y.S. Borghei, M. Hosseini, M.R. Ganjali, Fluorescence based turn-on strategy for determination of microRNA-155 using DNA-templated copper nanoclusters, Microchim. Acta 184 (2017) 2671–2677.
[20] Y. Luab, W. Chen, Sub-nanometre sized metal clusters: from synthetic challenges to the unique property discoveries, Chem. Soc. Rev. 41 (2012) 3594–3623.
[21] Y. Yuan, J. Zhang, G. Liang, X. Yang, Rapid fluorescent detection of neurogenin3 by CdTe quantum dot aggregation, Analyst 137 (2012) (1775).
[22] S. Kumar Kailasa, K.H. Cheng, H.F. Wu, Semiconductor nanomaterials-based fluorescence spectroscopic and matrix-assisted laser desorption/ionization (MALDI) mass spectrometric approaches to proteome analysis, Materials 6 (2013) 5763–5795.
[23] M. Hosseini, A. Akbari, M.R. Ganjali, M. Dadmehr, A.H. Rezayan, A novel label-free microRNA-155 detection on the basis of fluorescent silver nanoclusters, J. Fluoresc. 25 (2015) 925–929.
[24] Q. Xu, J.H. Wang, Z. Wang, Z.H. Yin, Q. Yang, Y.D. Zhao, Interaction of CdTe quantum dots with DNA, Electrochem. Commun. 10 (2008) 1337–1339.
[25] Y.S. Borghei, M. Hosseini, An approach toward miRNA detection via different thermo-responsive aggregation/disaggregation of CdTe quantum dots, RSC Adv. 8 (2018) 30148–30154.
[26] S. Anandampillai, X. Zhang, P. Sharma, G.C. Lynch, M.A. Franchek, K.V. Larin, Quantum dot–DNA interaction: computational issues and preliminary insights on use of quantum dots as biosensors, Comput. Methods Appl. Mech. Eng. 197 (2008) 3378–3385.
[27] J.J. Zhu, J.J. Li, H.P. Huang, F.F. Cheng, Quantum Dots for DNA Biosensing, Springer, 2013.
[28] F.O. Silva, M.S. Carvalho, R. Mendonça, W.A. Macedo, K. Balzuweit, P. Reiss, M.A. Schiavon, Effect of surface ligands on the optical properties of aqueous soluble CdTe quantum dots, Nanoscale Res. Lett. 7 (2012) 536.
[29] M. Hosseini, S. Mohammadi, Y.S. Borghei, M.R. Ganjali, Detection of p53 gene mutation (single-base mismatch) using a fluorescent silver nanoclusters, J. Fluoresc. 27 (2017) 1443–1448.
[30] W. Hui, S. Zhang, C. Zhang, Y. Wan, J. Zhu, G. Zhao, S. Wu, D. Xi, Q. Zhang, N. Li, Y. Cui, A novel lateral flow assay based on GoldMag nanoparticles and its clinical applications for genotyping of MTHFR C677T polymorphisms, Nanoscale 8 (2016) 3579–35787.
[31] H.L. Gao, M. Wang, Z.Q. Wu, C. Wang, K. Wang, X.H. Xia, A morpholino-functionalized nanochannel-array for label-free SNPs detection, Anal. Chem. 87 (2015) 3936–3941.
[32] S.L. Dodson, C. Cao, H. Zaribafzadeh, S. Li, Q. Xiong, Engineering plasmonic nanorod arrays for colon cancer marker detection, Biosens. Bioelectron. 63 (2015) 472–477.
[33] Y. He, D. Chen, M. Li, L. Fang, W. Juan, Y. Liang, J. Xu, F.F. Fu, Rolling circle amplification combined with gold nanoparticles-tag for ultrasensitive and specific quantification of DNA by inductively coupled plasma mass spectrometry, Biosens. Bioelectron. 58 (2014) 209–213.
[34] Y.T. Chin, E.C. Liao, C.C. Wu, G.J. Wang, J.J. Tsai, Label-free detection of single-nucleotide polymorphisms associated with myeloid differentiation-2 using a nanostructured biosensor, Biosens. Bioelectron. 49 (2013) 506–511.
[35] A. Singh, G. Sinsinbar, M. Choudhary, V. Kumar, R. Pasricha, H.N. Verma, S.P. Singh, K. Arora, Graphene oxide-chitosan nanocomposite based electrochemical DNA biosensor for detection of typhoid, Sensors Actuators B Chem. 185 (2013) 675–684.